AD-A128 993 WEIGHTING FOR THE MODULATION TRANSFER FUNCTION(U) NAVAL 1/1
POSTGRADUATE SCHOOL MONTEREY CA R J FLENNIKEN JUN 83

UNCLASSIFIED F/G 12/1 NL

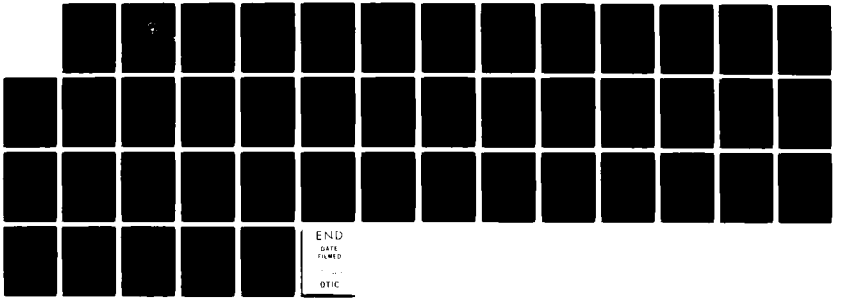

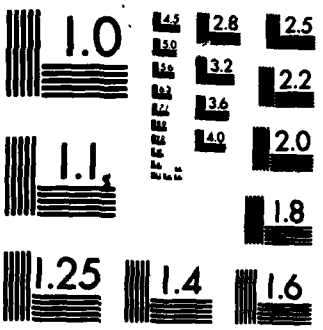

NAVAL POSTGRADUATE SCHOOL
Monterey, California

THESIS

WEIGHTING FOR THE MODULATION TRANSFER FUNCTION

by

Robert J. Flenniken

June 1983

Thesis Advisor: E. A. Milne

Unclassified

SECURITY CLASSIFICATION OF THIS PAGE (When Data Entered)

REPORT DOCUMENTATION PAGE		READ INSTRUCTIONS BEFORE COMPLETING FORM
1. REPORT NUMBER	2. GOVT ACCESSION NO. A128993	3. RECIPIENT'S CATALOG NUMBER
4. TITLE (and Subtitle) Weighting for the Modulation Transfer Function		5. TYPE OF REPORT & PERIOD COVERED Master's Thesis June 1983 6. PERFORMING ORG. REPORT NUMBER
7. AUTHOR(s) Robert James Flenniken		8. CONTRACT OR GRANT NUMBER(s)
9. PERFORMING ORGANIZATION NAME AND ADDRESS Naval Postgraduate School Monterey, California 93940		10. PROGRAM ELEMENT, PROJECT, TASK AREA & WORK UNIT NUMBERS
11. CONTROLLING OFFICE NAME AND ADDRESS Naval Postgraduate School Monterey, California 93940		12. REPORT DATE June 1983 13. NUMBER OF PAGES 44
14. MONITORING AGENCY NAME & ADDRESS(if different from Controlling Office)		15. SECURITY CLASS. (of this report) Unclassified 15a. DECLASSIFICATION/DOWNGRADING SCHEDULE

16. DISTRIBUTION STATEMENT (of this Report)

Approved for public release; distribution unlimited

17. DISTRIBUTION STATEMENT (of the abstract entered in Block 20, if different from Report)

18. SUPPLEMENTARY NOTES

19. KEY WORDS (Continue on reverse side if necessary and identify by block number)

Path weighting for index structure constant
Modulation transfer function

C sub n to the 2nd power

20. ABSTRACT (Continue on reverse side if necessary and identify by block number)

The effects of turbulence on the performance of imagers or on beam forming optical systems are well expressed by the optical transfer function (OTF) or its magnitude, the modulation transfer function (MTF). It has been shown that the MTF can be expressed in terms of the Fried model by means of a single number, the turbulence structure constants for optical index, C_n^2, provided that a properly path weighted value is obtained. Based on

(continued)

Item 20. (continued)

current theory the weighting needed in the path-position weighted value of C_n^2 is a function of $(z/z_o)^{5/3}$, heavily emphasizing the region near the imaging system or beam forming optics. It is the conclusion of this report, that the path weighting function $(z/z_o)^{5/3}$ is correct.

C SUB n TO THE 2ND POWER

Z SUB O) RAISED TO THE 5/3 POWER

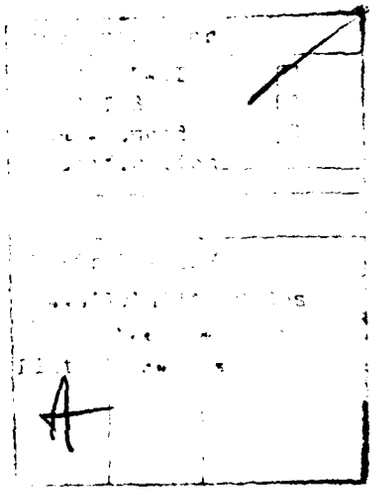

Approved for public release; distribution unlimited

Weighting for the Modulation Transfer Function

by

Robert J. Flenniken
Lieutenant Commander, United States Navy
B.S., University of Colorado, 1973

Submitted in partial fulfillment of the
requirements for the degree of

MASTER OF SCIENCE IN PHYSICS

from the

NAVAL POSTGRADUATE SCHOOL
June 1983

Author: Robert J. Flenniken

Approved by: Edmund A. Milne
Thesis Advisor

E. R. Crittenden, Jr.
Second Reader

G. E. Schacher
Chairman, Department of Physics

J. N. Dyer
Dean of Science and Engineering

ABSTRACT

The effects of turbulence on the performance of imagers or on beam forming optical systems are well expressed by the optical transfer function (OTF) or its magnitude, the modulation transfer function (MTF). It has been shown that the MTF can be expressed in terms of the Fried model by means of a single number, the turbulence structure constants for optical index, C_n^2, provided that a properly path weighted value is obtained. Based on current theory the weighting needed in the path-position weighted value of C_n^2 is a function of $(z/z_o)^{5/3}$, heavily emphasizing the region near the imaging system or beam forming optics. It is the conclusion of this report, that the path weighting function $(Z/Z_o)^{5/3}$ is correct.

TABLE OF CONTENTS

LIST OF FIGURES

I. INTRODUCTION

The quantity C_n^2, which varies with the micrometeorology, can be determined in its properly path-weighted form with the slit scanning telescope system developed at NPS by Crittenden et al (Crittenden, 1978). C_n^2 can also be computed from measurements of the temperature structure constant, C_t^2. Point measurements of C_t^2 are based on assumptions of the statistical form of the turbulence, while optical determination of C_n^2 with the slit-scanner is independent of this statistical nature.

Anomolies in the distribution of C_n^2 due to air flow around obstructions near the optics is a common problem. This has a direct naval application since for ship mounted optics, the heavily weighted part of the path is the shipboard end.

The objective of this work is to design and conduct an experiment to determine the path-weighted values of C_n^2 and compare these results to the existing model for the path weighting of the MTF. The model used is that proposed by the theoretical treatment of Fried (Fried, 1966) which predicts a $(Z/Z_o)^{5/3}$ dependence where Z_o = range.

II. THEORETICAL CONSIDERATIONS

A. GENERAL

Turbulence and temperature gradients in the atmosphere result in random fluctuations in temperature about an average value. Similarly, turbulence and humidity gradients result in humidity fluctuations. The optical index of refraction depends on both the temperature and the humidity, so that the index, n, undergoes fluctuations around its mean value.

A quantity useful in characterizing optical turbulence effects is the average of the square of the difference of the index of refraction at two points $\vec{r}$ and $\vec{r}$ separated by a distance r, i.e.,:

$$\langle [n(\vec{r}_1) - n(\vec{r}_2)]^2 \rangle$$

For isotropic turbulence, the quantity C_n^2, expressed by Tatarski (Tatarski, 1961):

$$\langle [n(\vec{r}_1) - n(\vec{r}_2)]^2 \rangle = r^{2/3} \quad C_n^2, \ \ell_o << r << L_o$$

is called the "index of refraction turbulence structure constant". This relationship holds within the "inertial sub-range",

$$\ell_o << r << L_o,$$

where ℓ_o and L_o are the inner and outer scales of turbulence respectively. These scales correspond roughly to the size of the smallest eddies of turbulence, about a millimeter, and the

largest eddies, often taken to be the order of the height above the surface of the point or propagation path of interest.

The quantity C_n^2 is a property at a point in the atmosphere. The mean of the integrated value of C_n^2 over the optical path, properly path weighted becomes the primary parameter of interest for the optical properties of the atmosphere due to turbulence.

Values of C_n^2 at specific points in the atmosphere can be measured from the temperature and humidity fluctuations. The index of refraction n, is related to the absolute temperature, T, by

$$n - 1 = 79 \times 10^{-6} \ p/T$$

with the pressure p in millibars. The average of the square of the temperature fluctuation can be shown to follow an equation similar to that for index fluctuation, leading to a definition of the temperature turbulence structure constant C_t^2 in terms of:

$$[T(\vec{r}_1) - T(\vec{r}_2)]^2 > = C_t^2 \ r^{2/3}$$

Using the expression for index in terms of p and T above, this leads to (Ochs, et al, 1969):

$$C_n^2 = [79 \times 10^{-6} \ (p/T^2)]^2 \ C_t^2$$

Earlier work at NPS (Crittenden, 1978) indicates that the contribution to the index variation from humidity fluctuations is small compared to temperature fluctuations and is therefore neglected in this report.

B. TURBULENCE EFFECTS ON OTF AND WANDER

Turbulence in the atmosphere, as expressed by a path-integrated C_n^2, determines the performance of imaging or beam-forming optical systems, and this performance can be used to measure the path-integrated C_n^2.

The effects of atmospheric turbulence on the performance of an imaging or beam projection system are usually treated (Fried, 1966; Lutomirski and Yura, 1974) by considering the atmosphere-plus-optics combination as a linear system, with the image being the response of the system to the object. If there were no sources of image degradation between the object and the image, a point object would have a point as its image. However, diffraction, caused by the finite aperture of the system, is always present. Within the present context, refraction and diffraction caused by the index of refraction inhomogeneities in the atmosphere are also present. These effects cause the ideal point response to a point object to be smeared out. If the point spread function has the same shape regardless of its position in the image plane, then the image function becomes the convolution of the object function and the point spread function. In this case the convolution theorem of Fourier transform theory yields:

$$i(\nu_x,\nu_y) = H(\nu_x,\nu_y) \cdot o(\nu_x,\nu_y)$$

where $i(\nu_x,\nu_y)$, $H(\nu_x,\nu_y)$, and $o(\nu_x,\nu_y)$ are the two-dimensional Fourier transforms of the image function, point spread function, and object function respectively and the values are the spatial frequencies. The quantity $H(\nu_x, \nu_y)$ is known as the optical transfer function (OTF) and its magnitude is called the modulation transfer function (MTF). The optical transfer function is thus the fundamental quantity which contains the effects of the atmopsheric turbulence. The modulation transfer function is also used to characterize the effects of turbulence, but it lacks information on phase.

For isotropic turbulence and circularly symmetric optics, the OTF is a function of $\nu_x = \nu_y = |\nu|$. In this case, a one-dimensional treatment is adequate. Physically, a one-dimensional image signal is obtained by scanning the image of a point object with a slit. Then the point spread function is replaced by the line-spread function:

$$h(x) = \int h(x,y)\, dy \quad \text{and} \quad i(\nu) = H(\nu)\, o(\nu)$$

Theoretical studies (Fried, 1966; Lutomirski and Yura, 1971) for an imaging system which include the effects of atmospheric turbulence show that the total optical transfer function can be expressed as the product of the transfer function for the optics and the transfer function for the atmosphere,

$$H_{tot}(\nu) = H_{opt}(\nu) \cdot H_{atm}(\nu)$$

Because of the stochastic nature of turbulence, quantities which relate to it can be understood only by means of an ensemble average. The problem of calculating the atmospheric MTF is considered in two limiting situations: the short term or short exposure (S.E.); and the long term or long exposure (L.E.). The short term MTF describes images obtained in the limit of time intervals sufficiently short that the turbulence can be considered frozen. The average short term MTF is then the average of the MTF's corresponding to many such images. The long term MTF results from taking an image of sufficiently long term which sees effectively all possible turbulence configurations. The average long term MTF is, therefore, the same as that from a single long time integrated exposure, since every turbulence configuration has been taken into account (properly weighted).

If one observes a series of line-spread images, one would find that each image is broadened over the diffraction limit imposed by the optics and that the center of the area of each image appears to wander. The first effect is called image spread and the second image wander. The short exposure MTF is obtained by taking the average (and then the Fourier transform) of successive line-spread functions in which each line-spread function is shifted so that the center of the area of each

curve has a common origin. This procedure removes the image wander. The long exposure MTF is obtained by not performing this shift in origin, therefore including image wander. The long exposure MTF is seen to be the result of image spread (the short term MTF) plus image wander.

Several theoretical models have been proposed from which the L.E. MTF can be derived. The only theoretical treatment of the S.E. MTF thus far is that of Fried (Fried, 1966). The result can be summarized by the following expression:

$$M(f) = \langle H(f) \rangle = \exp\left[-57.64\ \beta\ C_n^2\ z_o\ \lambda^{-1/3}\ f^{5/3}\left[1 - \alpha\left(\frac{f\lambda}{D}\right)^{1/3}\right]\right]$$

where

λ = wavelength

f = angular spatial frequency (cycles/radian), = $f\nu$

ν = linear spatial frequency (cycles/meter)

F = focal length of system

D = diameter of optics

z_o = range

$$\alpha = \begin{cases} 0 \text{ for the L.E. OTF} \\ 1/2 \text{ for the far-field S.E. MTF, } D << (z\lambda)^{1/2} \\ 1 \text{ for the near-field S.E. MTF, } D \gtrsim (z\lambda)^{1/2} \end{cases}$$

$$\beta = \begin{cases} 1 \text{ for a plane wave} \\ 3/8 \text{ for a spherical wave} \end{cases}$$

Use of this quantity, f, the angular spatial frequency appearing in this expression, avoids the necessity to know the

focal length or magnification of a system. Most experimental situations which employ a diverging laser beam as the light source or object can be considered to correspond to the spherical wave model. Plane waves are rarely encountered and will not be considered in this report.

C. PATH POSITION WEIGHTING OF C_n^2 FOR THE MTF

The expression (in the preceding section) for the MTF applies to the case where C_n^2 is independent of the position along the propagation path. If C_n^2 varies along the path, this equation generalizes for the L.E. spherical-wave MTF to

$$M(f) = \exp\left[-57.64\ \lambda^{-1/3}\ f^{5/3}\int_0^{z_o} C_n^2 \cdot (z/z_o)^{5/3}\, dz\right]$$

That is, C_n^2 is replaced by a weighted mean $\bar{C}_n^2$ given by

$$\bar{C}_n^2 = \frac{8}{3} \cdot \frac{1}{z_o} \int_0^{z_o} C_n^2 \cdot (z/z_o)^{5/3}\, dz$$

The experimentally determined MTF can be used to infer this weighted mean for C_n^2.

The above equation expresses the path weighting of C_n^2 indicated in Figure I-1 in which the path region nearest the imaging, or beam projecting system at $z = z_o$ has the largest contribution. The opposite end of the path has zero contribution.

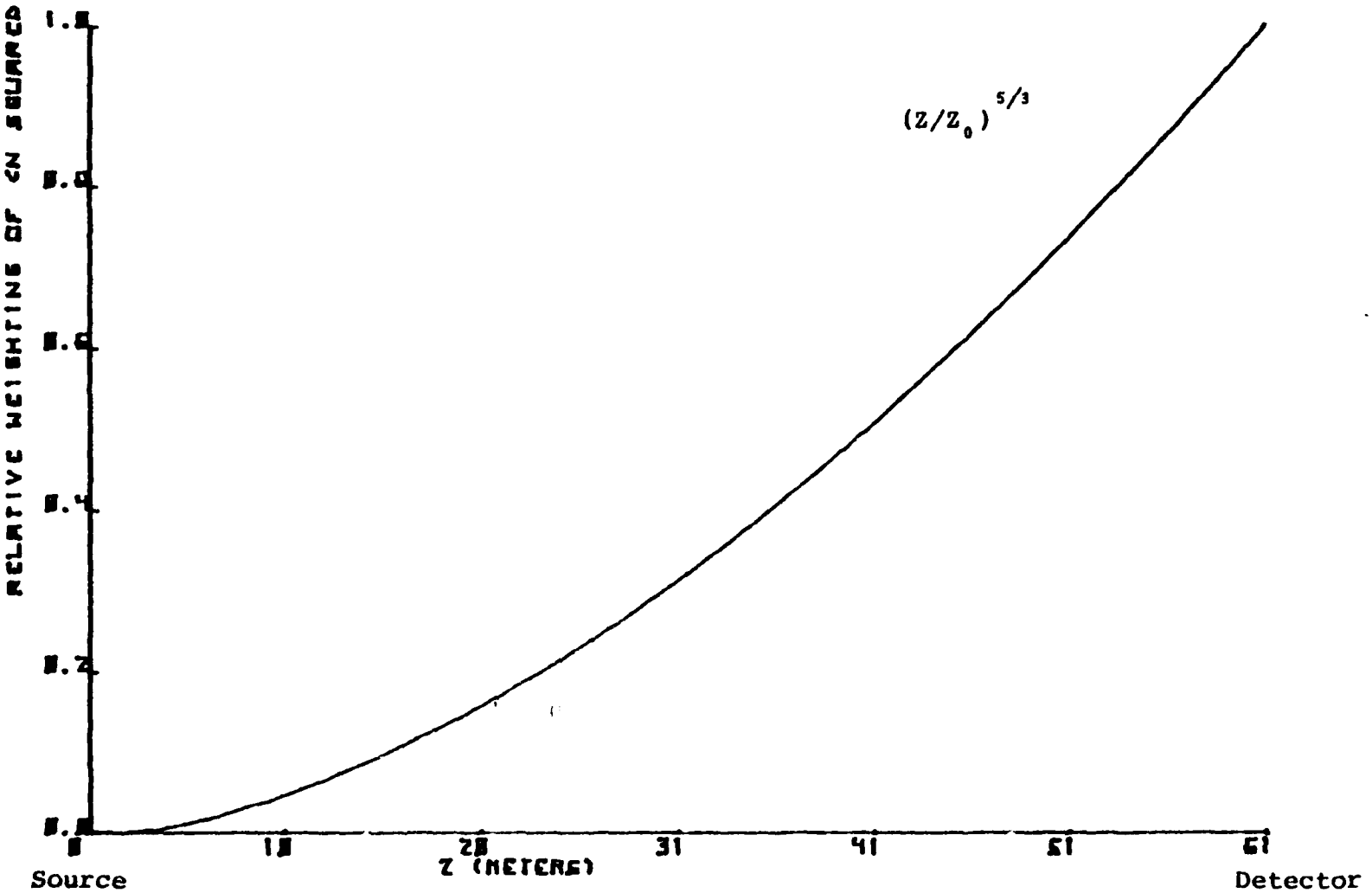

Figure II-1. Relative Path Weighting of C_n^2

III. GENERAL PLAN OF EXPERIMENTAL PROGRAM

A. GENERAL CONSIDERATIONS

The general objective is to confirm the path-weighting model for the MTF. If the background C_n^2 in a controlled environment is several orders of magnitude below the C_n^2 of a highly localized temperature disturbance, then the optically measured C_n^2 will be due primarily to the injected disturbance and the contribution of the remainder of the path may be ignored.

The major requirements of the experiment are then to construct an environment with sufficiently low and uniform background C_n^2 and to construct a heat source which adequately meets the isotropic turbulence requirements. This heat source will require a method of monitoring to ensure a nearly uniform disturbance as it is repositioned along the path in the controlled environment. If slight non-uniformities exist, they may be used as normalizing factors for the optically determined values of C_n^2.

B. PROCEDURE

A sixty-one meter tunnel was constructed for the controlled environment and a suitable heat source designed for the temperature disturbance. By placing the heat source at progressive locations in the "tunnel", measuring the optically determined values of C_n^2 from the MTF as determined by the slit-scanner and on-line data processing system, the results

were plotted as C_n^2 versus the temperature disturbance location in the tunnel. These are compared to the theoretical curves fitted to the data taken on the same graphs.

Monitoring of the heat source was achieved by using platinum temperature probes across an AC bridge to measure C_t^2 and thereby compute C_n^2 at the location of the temperature disturbance location. These values will not necessarily coincide with the optically determined values of C_n^2 due to their dependence on the statistical nature of the temperature of fluctuations of the heat source (micrometeorology). The optical measurements assume a uniform C_n^2 over the path. As mentioned earlier, the controlled environment ambient C_n^2 is much less than the C_n^2 of the heat source.

IV. MEASUREMENT TECHNIQUES

A. MTF

1. Long Term, Short Term, Wander

The performance of an imaging system, or of a beam projection system such as the HEL and pointer (tracker) can be characterized and predicted in terms of the MTF of the atmosphere. The experimental program has been designed to provide verification of the theoretical model for the path-weighting of the MTF.

As indicated in Section II, the MTF is expected to depend on the level of turbulence as expressed by the path-weighted value of C_n^2, and on the wavelength and range. Two experiments were carried out to determine the effect of a temperature disturbance on the path-weighting of the MTF. These have been carried out in a controlled environment as free from other turbulence as practicable with uniform values of C_n^2 over the path except at the points of interest.

Measurements of the MTF yield long term, short term, and wander. The internal consistency of these measurements are to be compared.

To calibrate the MTF in angular spatial frequency with a maximum scale of 500 microradians consisting of 1024 data points, a calibration signal is injected by placing a diffraction grating in front of the optics. The spacing between first order peaks is known to be 142.6 microradians, or $\lambda/d = 142.6/2 = 71.3$ microradians. The dwell time is the

number of microseconds per point. For a dwell time of 20, the time between the first order interference peaks

$= (20 \times 10^{-6}$ μsec/point) (1024 points) (142.6/500)

= 5.841 milliseconds

Using a Hewlett-Packard 1743 oscilloscope, this time is set on the calibration signal by adjusting the gain of the scanning mirror voltage. Center display of the signal is obtained by adjusting the scanning mirror D.C. offset.

The calibration grating is then removed and the desired signal observed.

A Wavetek model 145 function generator provides the sweep signal to the scanning mirror controller and a TTL output to an IEC P-12 pulse generator which provides a delayed trigger to the data processor NIC-80 described in section IV-2. This delayed trigger prevents the NIC-80 from seeing the sweep-back signal from the scanning mirror. Figure IV-1 diagrams the optical data processing equipment.

2. On-Line Data Reduction

The on-line data reduction unit is a Nicolet Instrument Company NIC-80 data processor. This is a data averager interfaced directly to Hewlett-Packard 9825B programmable calculator. The HP-9825B acts as the controller and input-output device to the NIC-80 and controls the plotter and printer.

The NIC-80 digitizes the analog signal from the detector, processes the raw data to obtain the experimental

MTF, wander and C_n^2. The processed experimental data is then transferred to the HP-9825B which is better suited for floating point calculations. The HP-9825B calculates the best fit curve and plots out the results in final form.

3. Optical Equipment

The optical equipment consists of an 8 inch diameter Celestron, Schmidt telescope with an equivalent focal length of 160 inches and an overall length of about 50 centimeters. It has a .344 central obscuration ratio. Mated to the image end of the telescope is the scanning mirror assembly. It consits of an optically flat mirror mounted on a servo motor to provide the sawtooth scan of the image across an adjustable slit. The mirror turns the optical path 90 degrees. The scan produces the line spread function as a function of time. A trigger signal associated with initiation of each scan indexes the position of the image.

The detector, mounted after the slit in the slit-scanner, is an RCA silicon photodiode type C30872. It is operated at 370 volts D.C. with a 9 volt battery powering the source follower. The detector used does not require cyrogenic cooling which is a large improvement in reliability and ease of use over a detector that did during earlier trials.

The telescope optics are supported on a rigid tripod base, weighted with 50 pounds of lead which prevents mechanical vibration of the telescope system. The optics and detector are sealed as a part of the tunnel during optical measurements.

The signal from the detector is preamplified by a high-gain, low-noise PAR 113 amplifier. The signal is processed immediately with the on-line equipment.

The source for the MTF system is a Helium-Neon laser transmitted from the far end of the tunnel. The laser beam passes through two polarizers to reduce its intensity and is diverged by a 10 centimeter lens to provide a spot size at the MTF telescope of about .5 meters wide. This provides uniform illumination over the aperture of the telescope and closely approximates light diverging as a spherical wave from a point source. The MTF telescope then images this point source. The laser is operated in the CW mode for this purpose. The laser wavelength utilized for MTF measurements is the red HeNe at 0.6328 micrometers.

4. Controlled Environment (Tunnel)

The tunnel was constructed of three-eighths inch construction plywood with completed sections measuring 2 feet by 2 feet by 8 feet (61 cm by 61 cm by 2.44 m). 25 tunnel sections were made for a tunnel length of 200 feet or 61 meters. Prior to construction an underseal of water repellant was applied both inside and out. The inside was then painted with flat black and the outside with an exterior white. The individual sections were constructed with 12 metal edge brackets, 8 end corner brackets, and 56 wood screws. The joints were sealed with a heavy duty tape to prevent air flow through any of the seams.

A special heat source tunnel section was built by modifying an existing section. An opening about 1 1/2 times the area of the heat source was cut in the top at one end and a 64 cm high chimney constructed over it. A wooden baffle sheet was placed over the top of the chimney (supported by small blocks) in a manner to allow air flow but prevent down drafts from entering the tunnel. A wide slit was cut in the bottom of the tunnel section under the chimney to allow for air flow across the heat source by convection. The slit was baffled to prevent entry of side drafts. Finally a small slit was cut in the side of the tunnel section for the insertion of the platinum temperature probes above the heat source. The heat source was then placed under the chimney in the bottom of the tunnel section (Figure IV-2).

The tunnel, located in the basement of Spanagel Hall at NPS, was assembled for the experimental runs only after working hours since it blocks several doorways and was disassembled after each run. When assembled, the joining and sealing of tunnel sections was achieved by taping. During the experimental runs, the heat source was injected every other tunnel section or every 4.88 meters along the 61 meter path.

A table was positioned at each end of the tunnel to house the optics and detector at one end and the laser and lenses at the other. During the runs, these tables were sealed and became an integral part of the tunnel's controlled environment.

If the tunnel were a perfect controlled environment with no temperature disturbances, a point source at one end would be imaged by the optics as a point source at the other end and the MTF would be a straight line (normalized $C_n^2 = 1$ independent of spatial frequency). Figure IV-3 shows the very high degree of "perfection" achieved for the controlled environment inside the tunnel.

5. Heat Source

As discussed in Section II, a region of isotropic turbulence for $\ell_o << r << L_o$ is required (or approximately so) from whatever heat source would be used. In this region C_n must be reasonably uniform. For several heat sources the C as a function of r (the probe spacing for the C_n^2 from C_t^2 equipment described in Sections V-B and C) was plotted. The heat section used gave the best results and the data is displayed in Figure IV-4.

The heat source consists of a two conductor heating element bent in reversing V's mounted on a wooden stand with ceramic standoffs. The wide spacings of the elements were to assist in providing the larger turbulence size which was considered to be about the height of the probes above the heat source, 22 cm (Lo). A screen of wire spacing .15 cm was placed over the heating element to provide the smaller turbulence size (ℓ_o).

Power was supplied by a Variac set at 70 volts AC which produced a temperature 22 centimeters above the heat source of about 27-30 Celsius.

Assuming $\ell_o << r_o << L_o$ or .15 cm <<r<< 22 cm the region of isotropic turbulence would be expected to be in the vicinity of 1.5 to 2.5 centimeters. Figure IV-4 shows a peak around 2.0 centimeters the remainder of the curve falling off as $r^{1/3}$ (the path dependence of C_n). The 2 centimeter region was considered to be approximately isotropic. A probe spacing of 6 centimeters was eventually decided upon due to the sharp peak at 2 centimeters. A more linear section of the curve is desired for more uniform results since the measured C_n^2 will be used to monitor the stability of the heat source and provide weighting for the optically determined results.

Thus decided upon, the heat source was placed in the bottom of the special tunnel section designed for it (Figures IV - 5 and 6).

B. C_t^2 POINT DETERMINATION

To determine C_t^2,

$$C_t^2 = <[T(r_1) - T(r_2)]^2> r^{-2/3}$$

T must be measured. The value of r, the temperature probe spacing in meters has been picked at .06 meters as discussed in the previous section.

Using two platinum wire temperature probes, ($\alpha = .0036° K^{-1}$) each with a resistance of approximately 56 ohms, across an AC Bridge, the output is cailbrated for ΔT. The bridge sensitivity was set and measured at 6.67 volts/ohm.

$$\Delta T \text{ per volt} = \frac{1}{(.0036\ ^{\circ}K^{-1})(56\ \text{OHMS})(6.67\ \text{Volt/OHM})}$$

ΔT per volt = .744 K per volt.

Using a spectrum analyzer on the ΔT fluctuations, the half power point for the ΔT fluctuations was determined to be about 8 hertz. A Hewlett-Packard 3438 A System Voltmeter, sampling at an 11 hertz rate for 500 samples (45 seconds), is then used to determine the values of ΔT. The system voltmeter is controlled by a Hewlett-Packard 9825B programmable calculator. It squares each ΔT sample and averages the 500 squared samples. Multiplying by $r^{-2/3}$, the calculator outputs C_t^2.

C. C_n^2 FROM C_t^2

To determine C_n^2 ,

$$C_n^2 \left[79 \times 10^{-6} \ (P/T^2)\right]^2 C_t^2$$

the absolute temperature of the heat source must be measured.

Using a Copper-Constantan thermocouple referenced to 0° Celsius (ice water) and sampling at a 3 hertz rate using a Hewlett-Packard 3490A multimeter controlled by the Hewlett-Packard 9825B calculator, forty samples of temperature are taken and averaged. Twenty are before the sampling for C_t^2 and twenty after.

T = <Thermo-Couple Voltage> 32809.524 °C per volt. Adding 273.15 gives the temperature in degrees Kelvin.

Assuming a constant atmospheric pressure of 1013.25 millibars, the H/P 9825B calculates C_n^2 to be used for monitoring the heat source and weighting of the optically determined values of C_n^2 .

Figure IV-7 shows a block diagram of the equipment used in the C_t^2 , T and C_n^2 measurements and calculations.

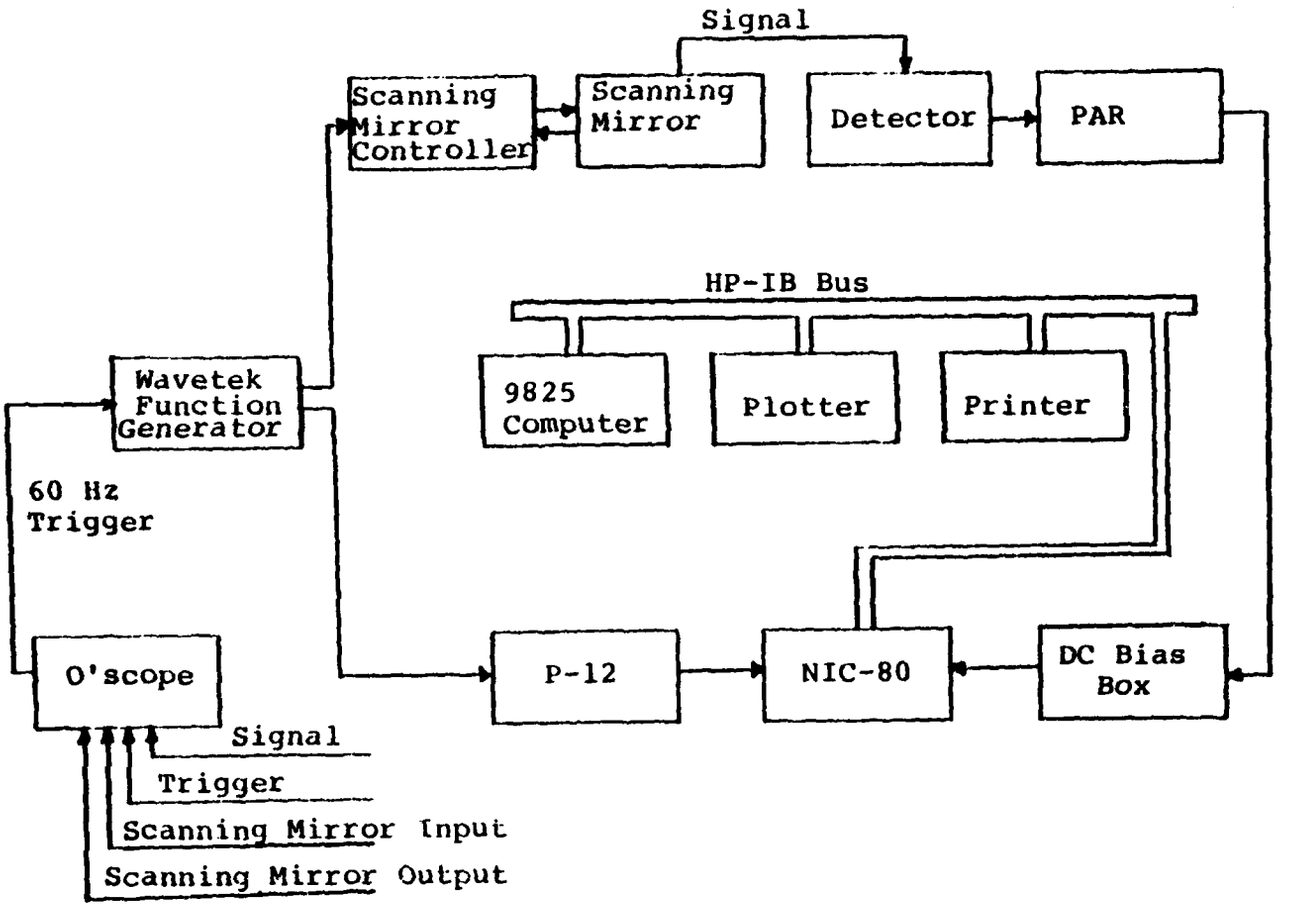

Figure IV-1. Optical Data Processing Equipment

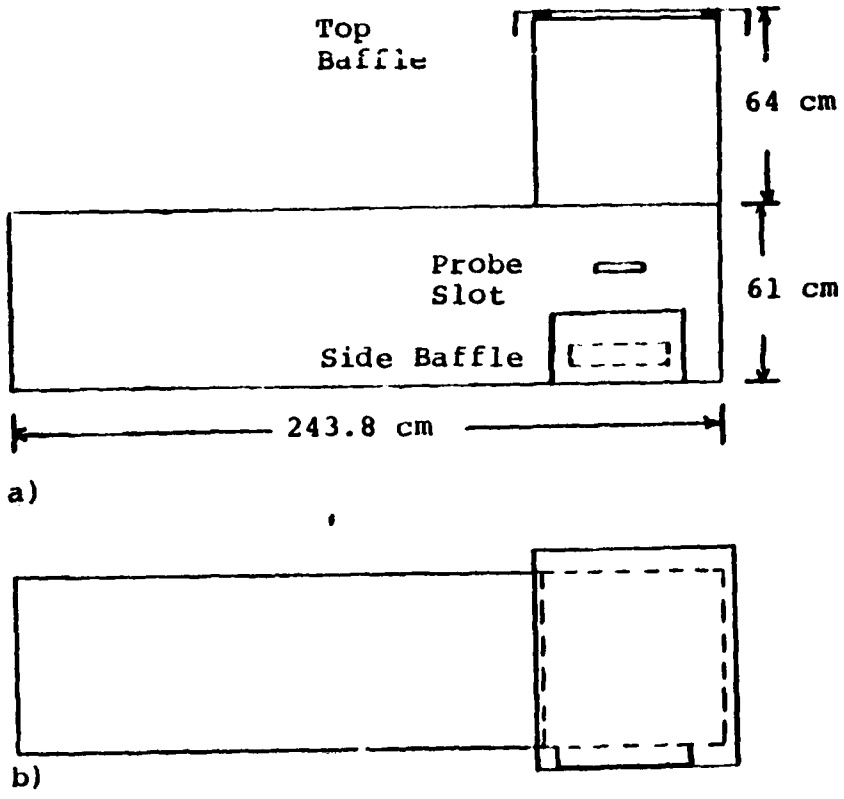

Figure IV-2. Tunnel Heat Source Section.
a) Side view
b) Top view

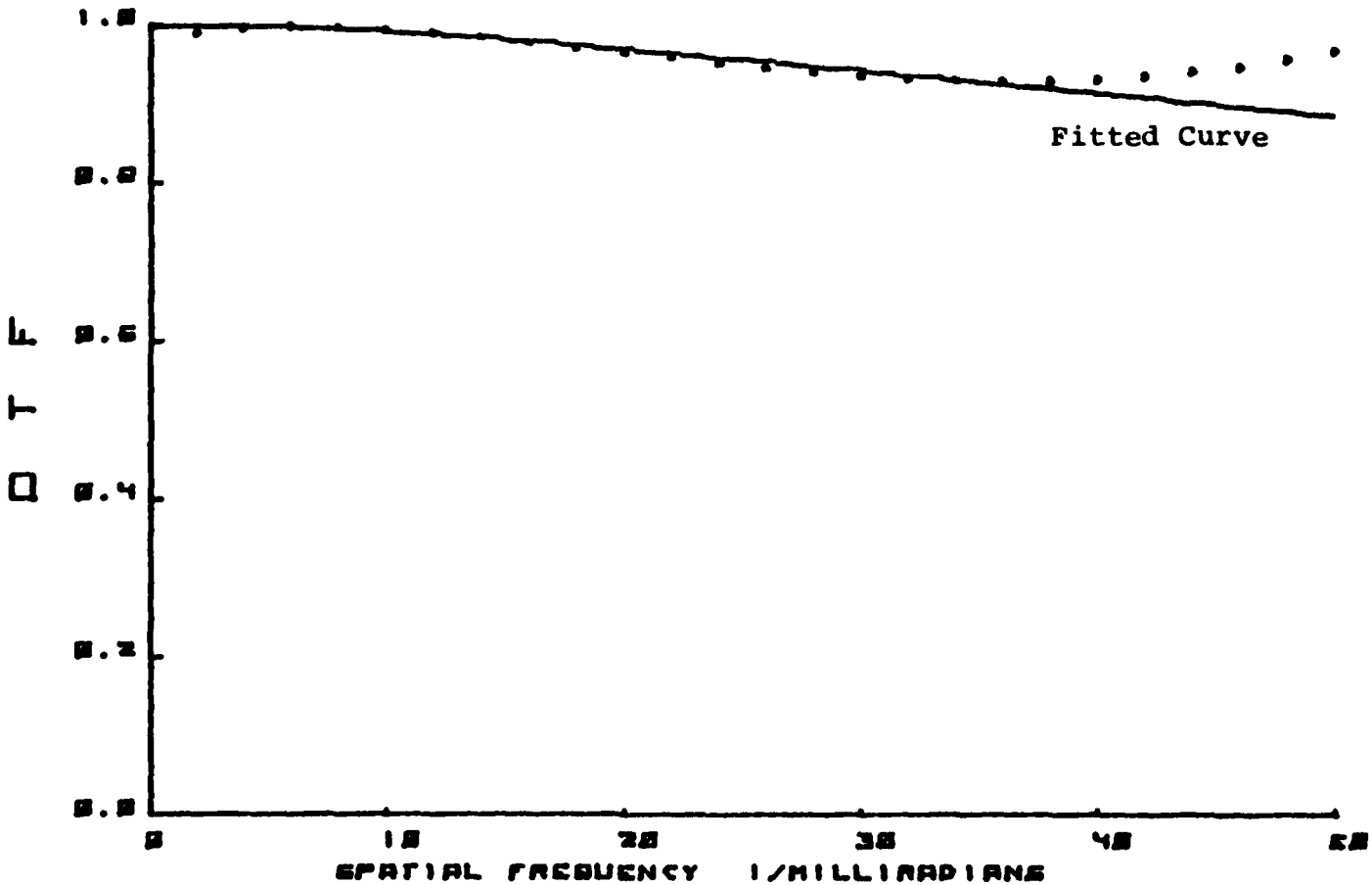

Figure IV-3. OTF of the Sealed Tunnel with No Heat Source Present

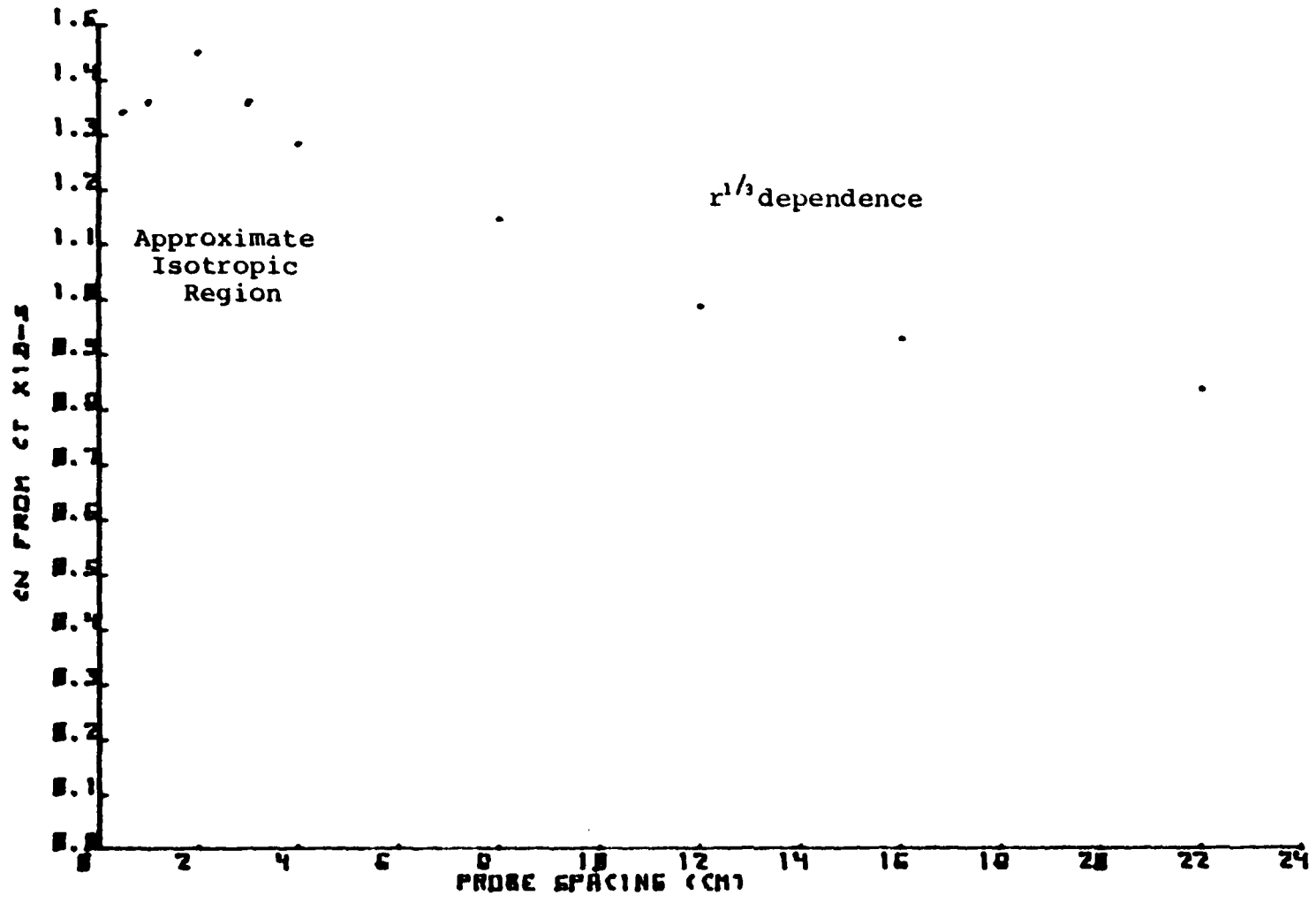

Figure IV-4. Isotropic Turbulence Region Determination

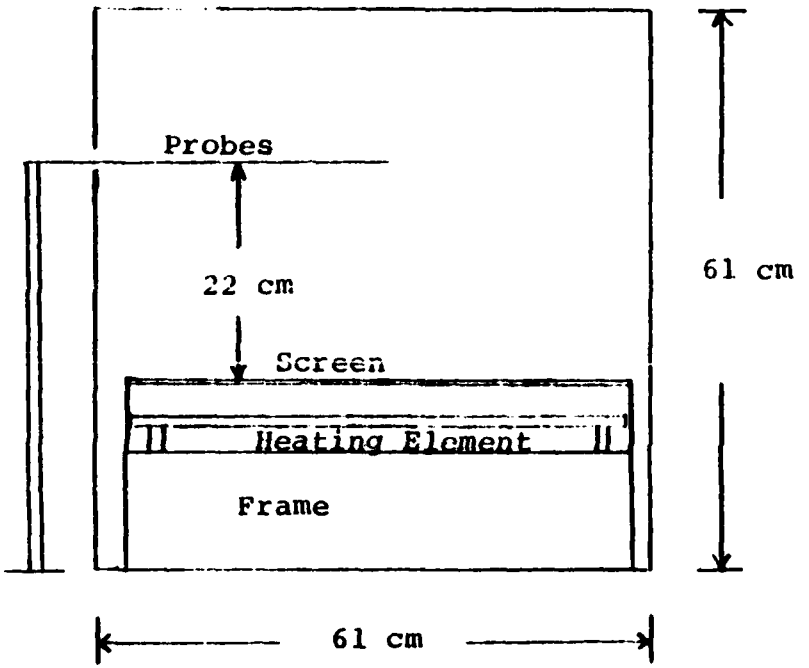

Figure IV-5. End View of Heat Source Tunnel Section

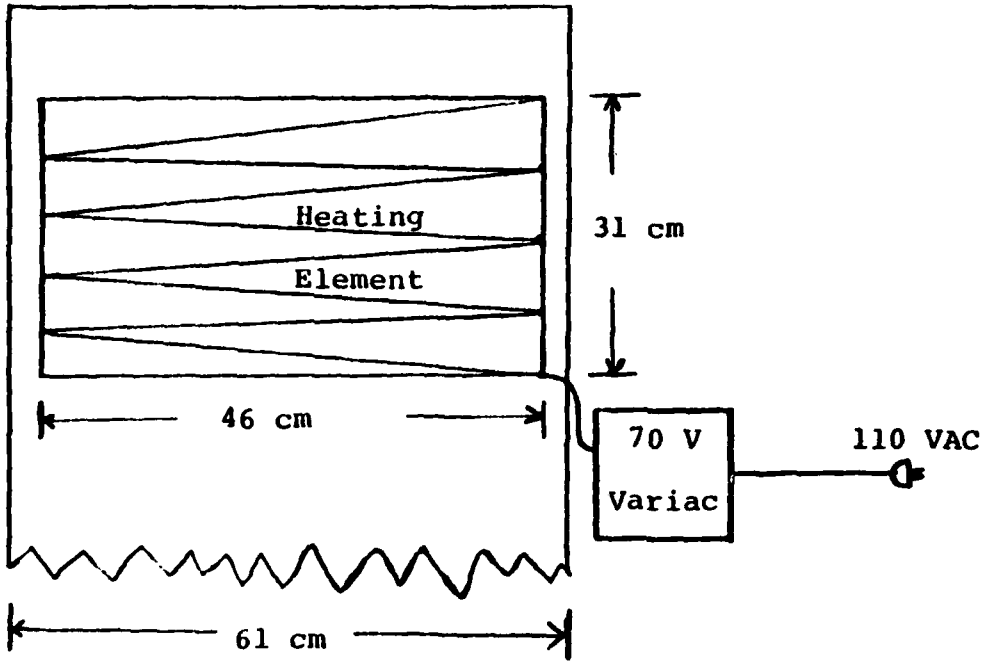

Figure IV-6. Heating Element Configuration

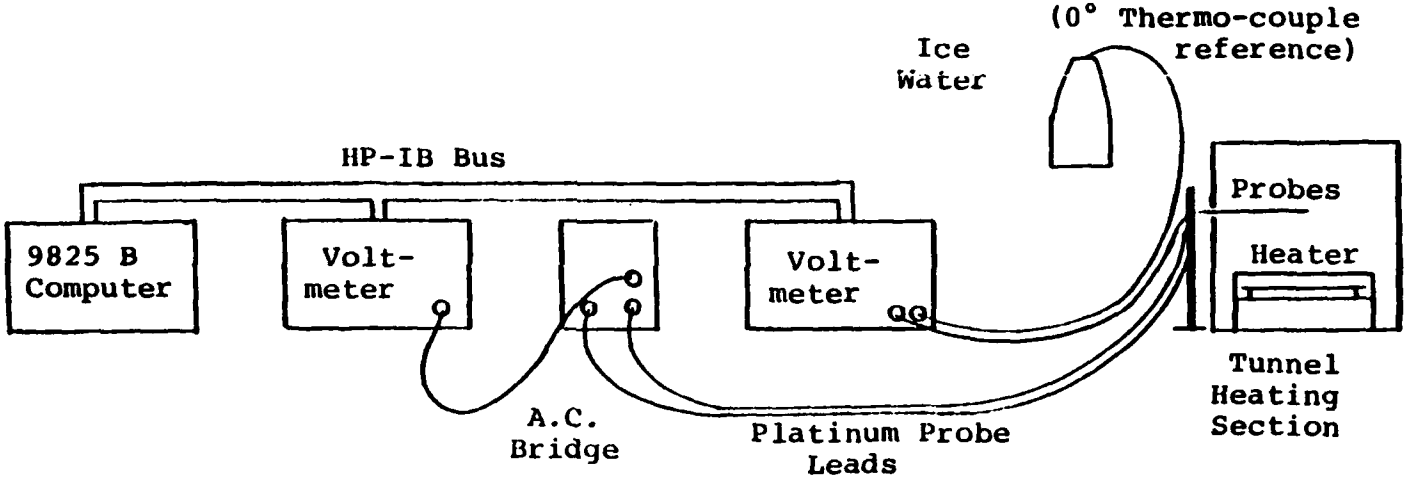

Figure IV-7. Equipment Used for Point C_t^2 Measurement and C_n^2 Calculations

V. RESULTS

A. EXPERIMENTAL DATA

1. 22 March 1983

During the evening of 22 March 1983, the first experimental run was made in the basement of Spanagel Hall at NPS. A "quiet" tunnel result similar to Figure IV-3 was obtained confirming the quality of the tunnel's environment. The point values of C_n^2 from C_t^2 were fairly uniform along the path with an apparent systematic increase on the detector end of the tunnel. The short term results (Figure V-1) were in excellent agreement with theory but the long term results (Figure V-2) though good, were not as convincing. The results from wander (omitted) were totally random in appearance.

Since wander is the shift in image center, vibrations could cause these erratic results. The initial telescope mount was not the one described in Section IV-A, 2. The original mounting was noted as being susceptible to vibration and the wander data on this run motivated its alteration.

2. 11 April 1983

After the telescope vibration problem was corrected, a second experimental run was conducted during the evening of 11 April 1983 in the same location.

C_n^2 from C_t^2 point values (Figure V-3) were very uniform over the path. Again the short term results (Figure V-4) were in excellent agreement with theory while the long term results

(Figure V-5) were not as good, but still showed the general shape of the curve. The wander results (Figure V-6), though vastly improved, cannot be used to substantiate the theoretical model.

B. ANALYSIS OF DATA

The following conclusions are drawn from the experimental data:

1. The short term results confirm the Fried model for the path-weighting of the MTF.
2. The long term results give good credibility to the Fried model, but cannot be used to positively confirm it.
3. The wander results do not support the theoretical model.

The overall conclusions is that the Fried model is correct and that systematic noise is responsible for the poor quality of the wander results and aberrations in the long term results. As described earlier, wander is not removed during the processing of the long term data so any physical or electrical vibration of the experimental system will affect the wander primarily and the long term to a lesser degree.

C. RECOMMENDATIONS

Since lead bricks weighted all physical components of the system, the likelihood of mechanical vibrations during the second run is low.

A large source of possible error seems to be in the sweep generation of the scanning mirror. The flatness of the

sawtooth sweep voltage was adjusted by eye. To ensure linearity over the sampling region of the sweep, the Fourier transform of the ramp function could be computed and compared to a spectrum analysis of the scan-mirror output signal. Any deviation from the predicted components would be a source of mirror vibration and hence, wander.

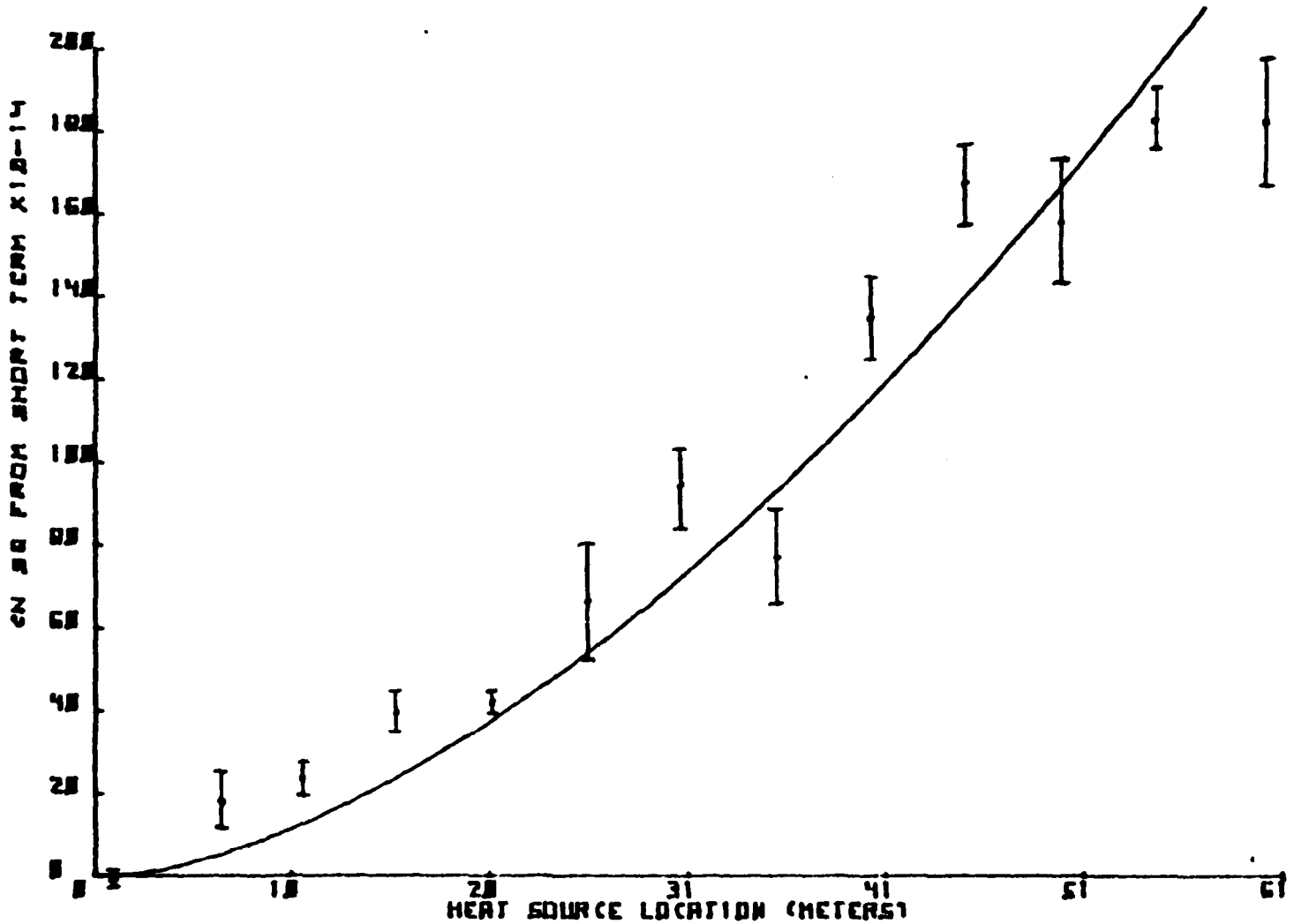

Figure V-1. Short Term Path-Weighting for MTF (22 March 1983)

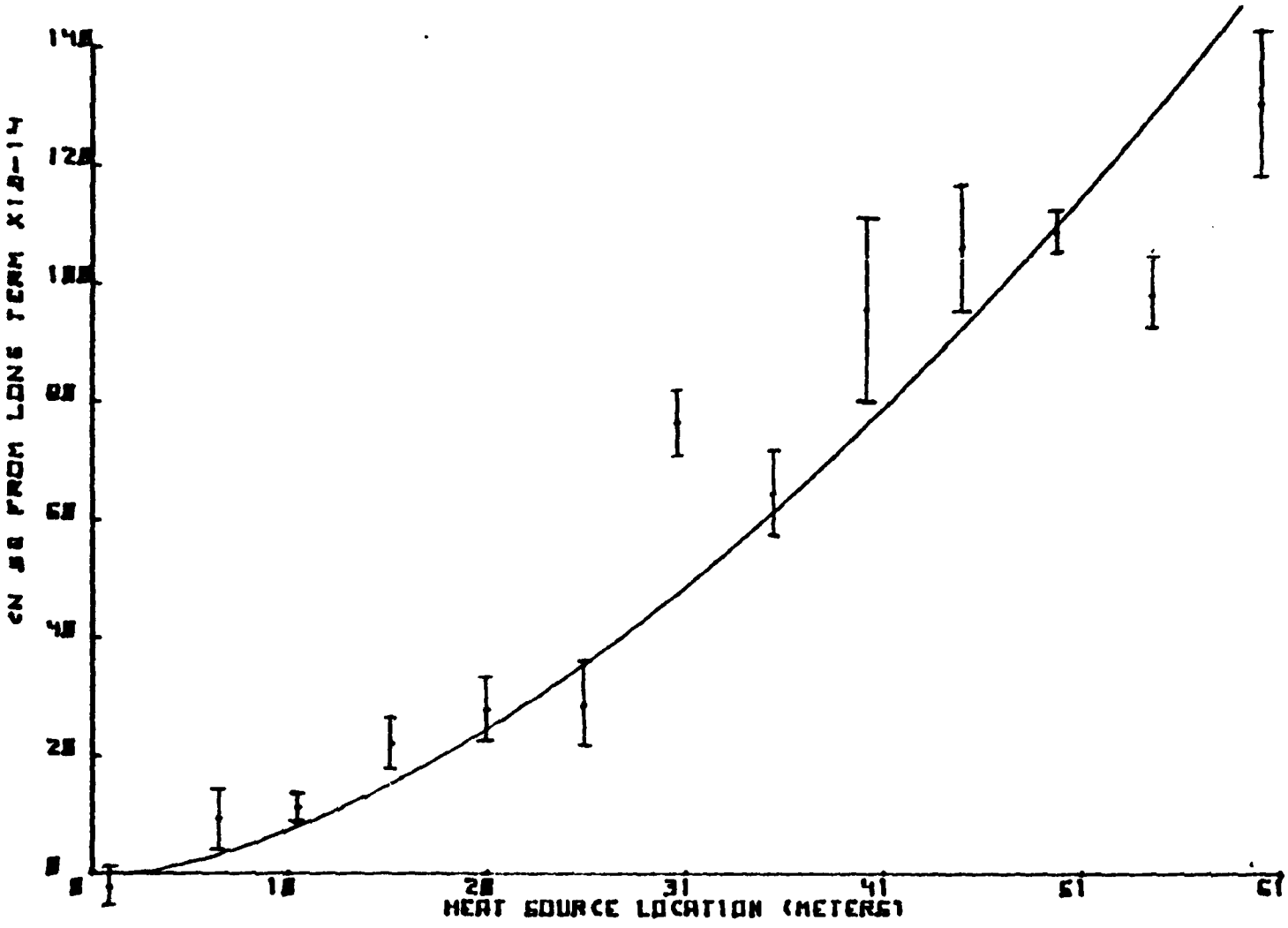

Figure V-2. Long Term Path Weighting for MTF (22 March 1983)

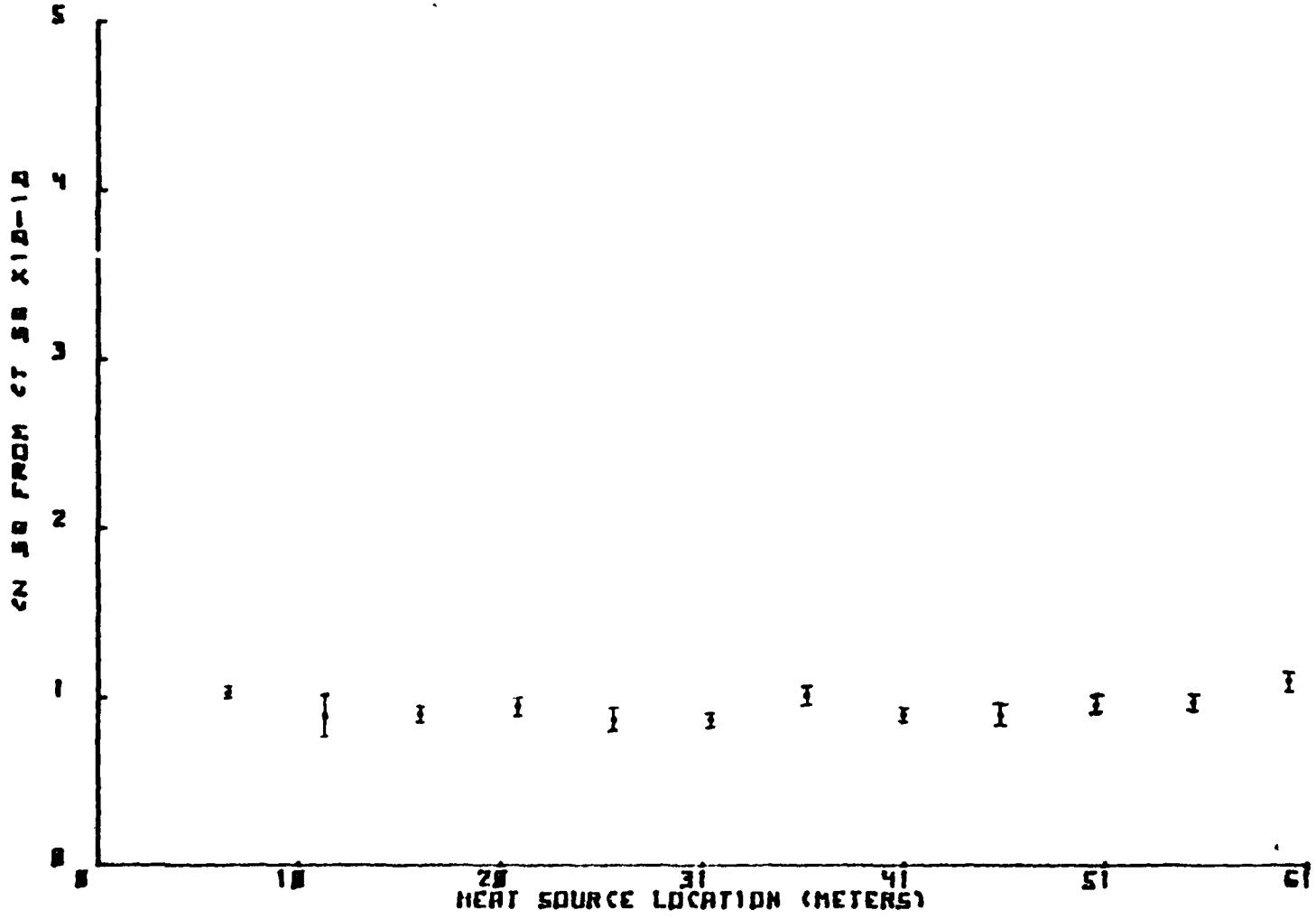

Figure V-3. C_n^2 From C_t^2 for the heat source over the Optical Path (11 April 1983)

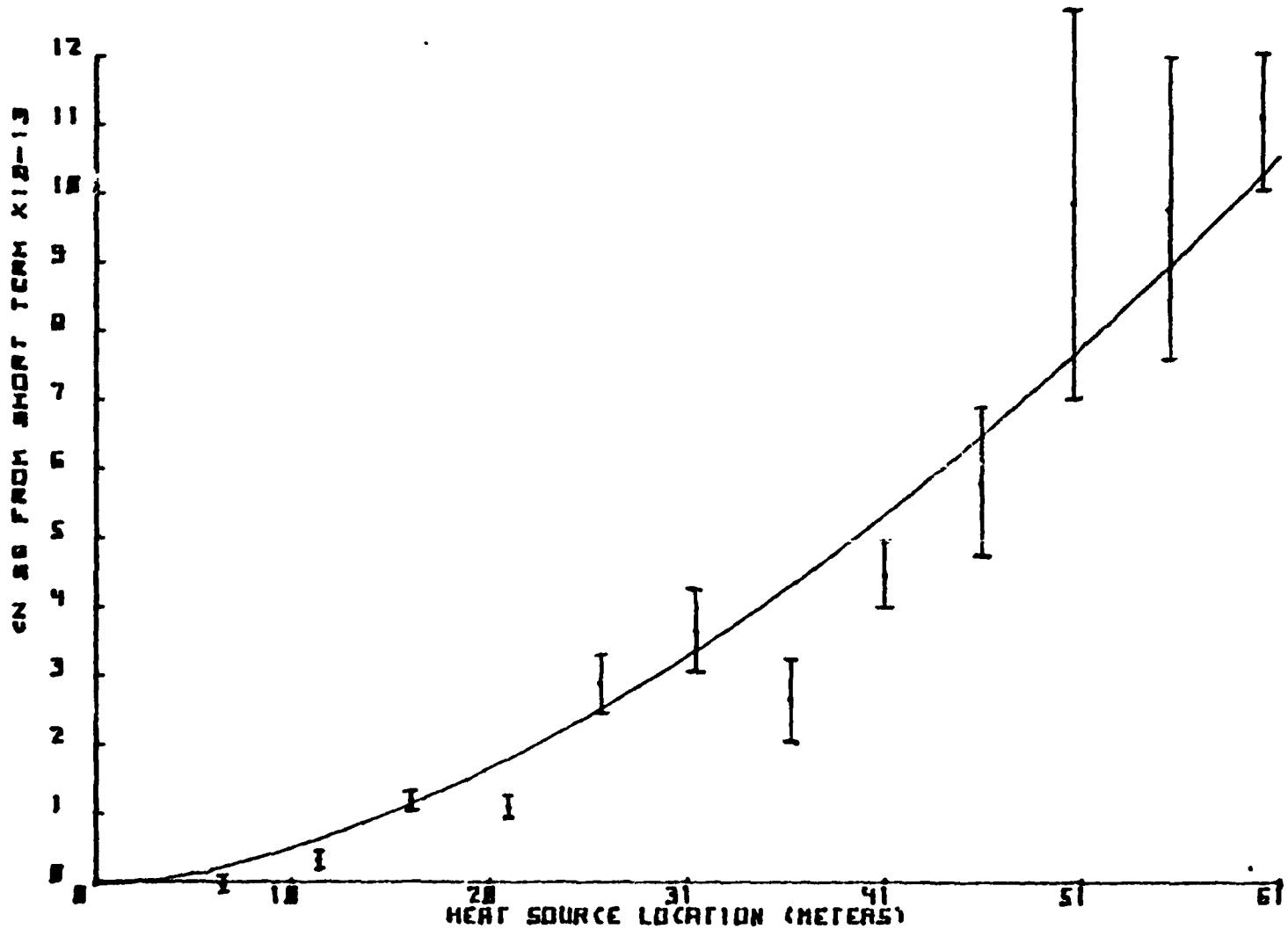

Figure V-4. Short Term Path Weighting for MTF (11 April 1983)

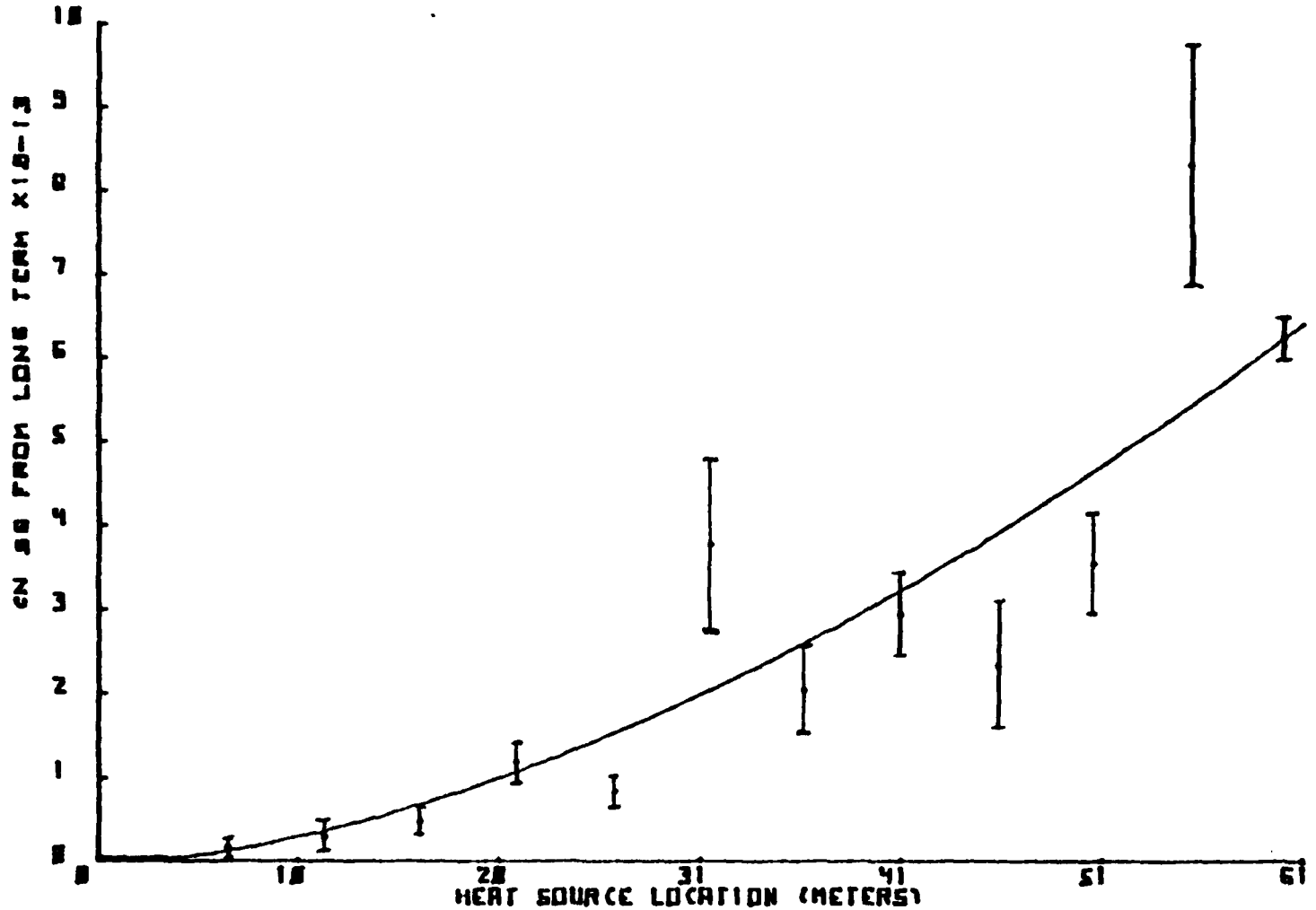

Figure V-5. Long Term Path Weighting for MTF (11 April 1983)

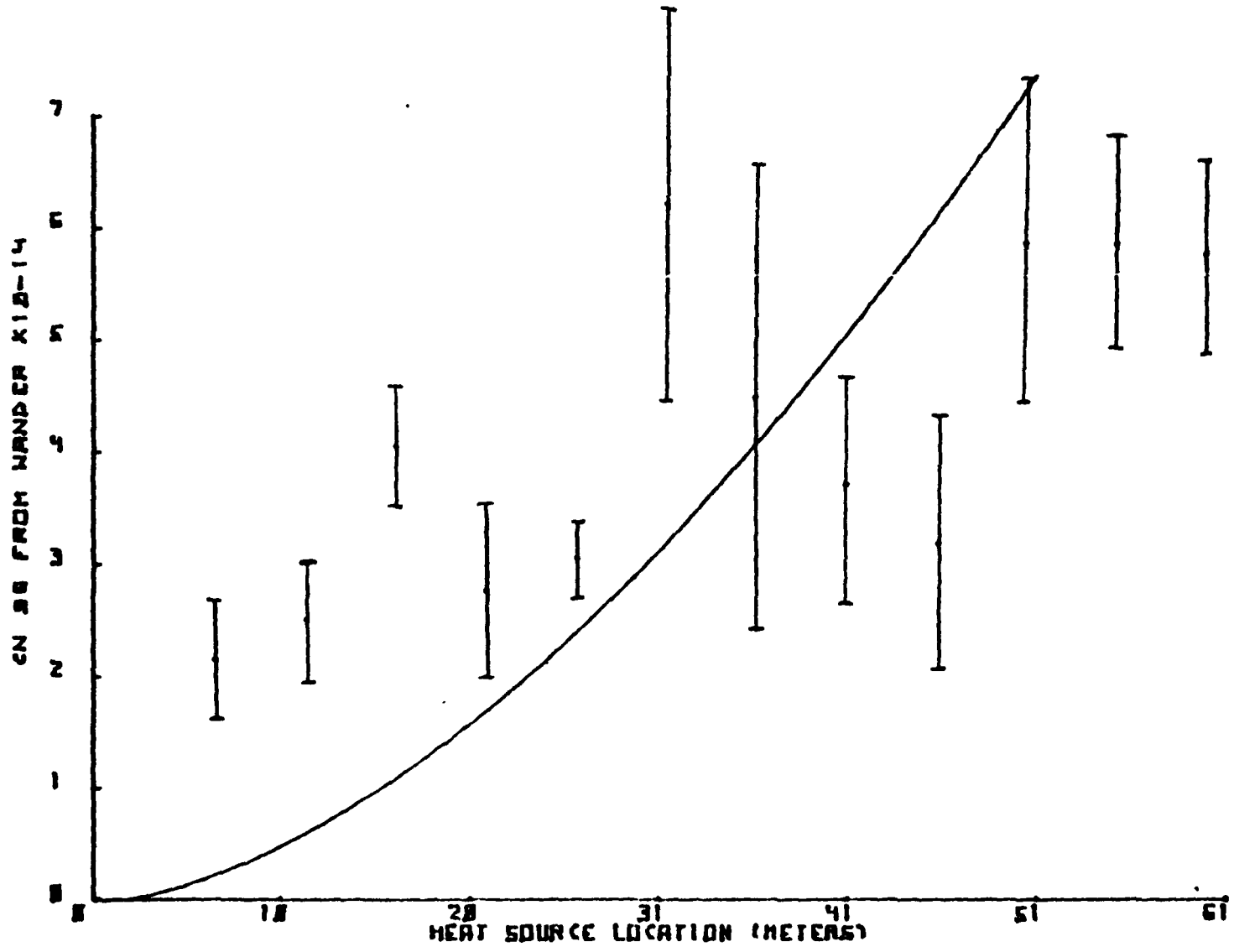

Figure V-6. Wander Path Weighting for MTF (11 April 1983)

LIST OF REFERENCES

Crittenden, 1978; Crittenden, E.C. Jr., Cooper, A. W., Milne, E. A., Rodeback, G. W., Armstead, R.L., Kalmback, S. H., Land, D., Katz, B., Optical Resolution in the Turbulent Atmosphere of the Marine Boundary Layer.

Fried, 1966; Fried, D. L., Optical Resolution Through a Randomly Inhomogeneous Medium for Very Long and Very Short Exposures, Jour. Optical Soc. Am., 56, 10, 1732, 1966.

Lutomirski, 1971; Lutomirski, R. F., and Yura, H. T., Propagation of a Finite Optical Beam in an Inhomogeneous Medium, Applied Optics, 10, 1652, 1971.

Lutomirski, 1974; Lutomirski, R. F., and Yura, H. T., Imaging of Extended Objects through a Turbulent Atmosphere, Applied Optics, 13, 431, 1974.

Ochs, 1969; Ochs, G. R., Bergmann, R. R., and Snyder, J. R., Laser Beam Scintillation Over Horizontal Paths from 5.5 to 145 kilometers, Jour. Optical Society Am., 59, 2, 231, 1969.

Tatarski, 1961; Tatarski, V. I., Wave Propagation in a Turbulent Medium (McGraw-Hill Book Company, Inc., New York, 1961;) The Effects of the Turbulent Atmosphere on Wave Propagation (U.S. Department of Commerce, NTIS, Springfield, Virginia 1971).

INITIAL DISTRIBUTION LIST

		No. Copies
1.	Defense Technical Information Center Cameron Station Alexandria, Virginia 22314	2
2.	Library, Code 0142 Naval Postgraduate School Monterey, California 93940	2
3.	G. E. Schacher, Chairman, Code 61Sq Department of Physics Naval Postgraduate School Monterey, California 93940	2
4.	E. C. Crittenden, Jr., Code 61Ct Department of Physics Naval Postgraduate School Monterey, California 93940	2
5.	Professor E. A. Milne, Code 61Mn Department of Physics Naval Postgraduate School Monterey, California 93940	4
6.	G. W. Rodeback, Code 61Rk Department of Physics Naval Postgraduate School Monterey, California 93940	2
7.	M. C. Drong, Code 1230 Pacific Missile Test Center Point Mugu, NAS, California 93042	1
8.	A. G. Costantine Department of Physics USMA West Point, NY 10996	1
9.	R. J. Flenniken So. 1017 Wright Blvd Liberty Lake, Washington 99019	2
10.	Captain David Anhalt, Code 1230.2 Pacific Missile Range Point Mugu, NAS, California 93042	1

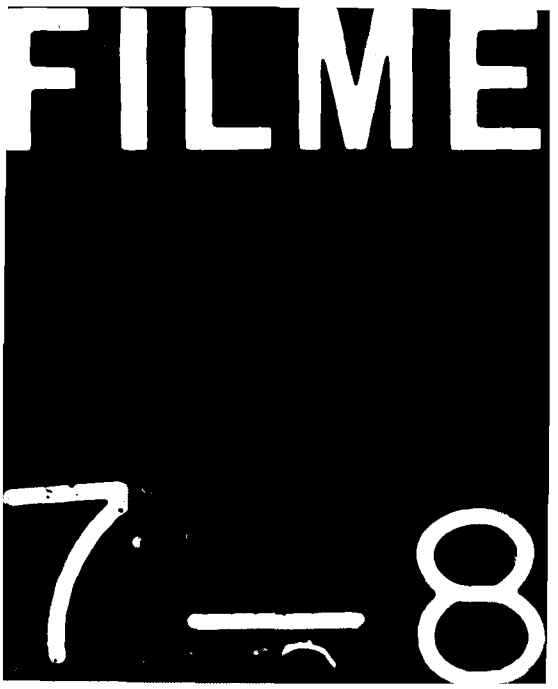
FILME
7—8